PHYSICAL REVIEW C **89**, 031602(R) (2014)

Neutron-capture cross-section measurements of ^{136}Xe between 0.4 and 14.8 MeV

Megha Bhike and W. Tornow
Department of Physics, Duke University, Durham, North Carolina, 27708, USA
and Triangle Universities Nuclear Laboratory, Durham, North Carolina, 27708, USA
(Received 4 February 2014; published 24 March 2014)

Fast-neutron-capture cross-section data on ^{136}Xe have been measured with the activation method between 0.4 and 14.8 MeV. The cross section was found to be of the order of 1 mb at the eleven energies investigated. This result is important to interpret potential neutron-induced backgrounds in the enriched xenon observatory and KamLAND-Zen neutrinoless double-β decay searches that use xenon as both source and detector. A high-pressure sphere filled with ^{136}Xe was irradiated with monoenergetic neutrons produced by the reactions ^{3}H$(p,n)^{3}$He, ^{2}H$(d,n)^{3}$He, and ^{3}H$(d,n)^{4}$He. Indium and gold monitor foils were irradiated simultaneously with the ^{136}Xe to determine the incident neutron flux. The activities of the reaction products were measured with high-resolution γ-ray spectroscopy. The present results are compared to predictions from ENDF/B-VII.1 and TENDL-2012.

DOI: 10.1103/PhysRevC.89.031602 PACS number(s): 25.40.Lw, 24.10.Pa, 28.20.Np, 95.55.Vj

The isotope ^{136}Xe has been considered as one of the most promising candidates for neutrinoless double-beta decay ($0\nu\beta\beta$) due to its large Q value and its ideal characteristics for use in large-scale experiments. The experiments named "enriched xenon observatory" (EXO) [1] located at the Waste Isolation Pilot Plant (WIPP) in Carlsbad, New Mexico, USA, and the Kamioka liquid scintillator antineutrino detector zero electron neutrino (KamLAND-Zen) [2] at the Kamioka mine in Japan are currently taking data. Combining the available results from these two experiments provides the lowest upper limit for the electron antineutrino mass of $<$120 to 150 meV [2]. Here, the uncertainty range of the neutrino-mass expectation value is mostly due to the uncertainty in the calculated nuclear matrix element [3]. However, pushing the present limit to considerably lower values or even to the potential discovery of $0\nu\beta\beta$ is a very challenging task. Although these experiments operate underground, neutron-induced background reactions will become a major concern, because they could potentially produce γ-ray radiation at the energy of interest for $0\nu\beta\beta$, i.e., 2458 keV for ^{136}Xe. Here, the neutrons are either produced by muon-induced spallation reactions or by (α,n) reactions in the detector material itself or its associated shielding. In order to reliably predict the amount of neutron-induced background in these experiments, the relevant cross sections must be known, as well as the neutron flux at the location of the experiment.

Recently, data for the ^{136}Xe$(n,2n)^{135}$Xe reaction have been published, and the importance of the ^{136}Xe$(n,\gamma)^{137}$Xe capture reaction has been pointed out [4]. The beta decay of ^{137}Xe to ^{137}Cs results in a number of deexcitation γ rays with energies in the vicinity of the ^{136}Xe $0\nu\beta\beta$ Q value. As described in Ref. [4], the γ rays at 2463.3 and 2474.8 keV are of concern for EXO, while for KamLAND-Zen the γ rays at 2422.7, 2444.0, 2452.4, 2474.8, and 2490.4 keV have to be considered in addition.

Experimental data for the ^{136}Xe$(n,\gamma)^{137}$Xe capture cross section are very scarce. Results of four measurements at thermal energies were published in Refs. [5–8]. At these low energies the cross section is as high as 5 b. Beer *et al.* reported a cross-section result of 1.05 ± 0.09 mb at 0.0375 MeV by using neutrons produced via the reaction ^{7}Li$(p,n)^{7}$Be [9]. Finally Hughes *et al.* used unmoderated fission neutrons to measure the ^{136}Xe$(n,\gamma)^{137}$Xe cross section at an effective energy of 1 MeV, resulting in a value of 1 mb, the only datum in the MeV energy regime [10]. Therefore, any estimates of background caused by neutrons with energies above 1 MeV in $0\nu\beta\beta$ experiments involving ^{136}Xe must rely on model calculations for the important ^{136}Xe$(n,\gamma)^{137}$Xe capture reaction cross section.

In order to provide experimental data and to guide model calculations, the ^{136}Xe$(n,\gamma)^{137}$Xe cross section was measured with monoenergetic neutrons in the 0.4 to 14.8 MeV energy range. In the following the experimental approach is described and the results are presented in comparison to existing model calculations.

The neutron activation of ^{136}Xe was carried out using the 10 MV model FN Tandem Accelerator at the Triangle Universities Nuclear Laboratory (TUNL). Monoenergetic neutron beams were produced at six energies in the range from 0.4 to 3.5 MeV via the ^{3}H$(p,n)^{3}$He reaction ($Q = -0.764$ MeV), at four energies between 4.1 and 7.31 MeV by using the ^{2}H$(d,n)^{3}$He reaction ($Q = +3.27$ MeV), and finally at 14.79 MeV by employing the ^{3}H$(d,n)^{4}$He reaction ($Q = +17.59$ MeV). Enriched xenon gas (99.9%) of mass 725 mg and pressurized to 250 atm was contained in a titanium sphere with inner diameter of 0.96 cm and wall thickness of 0.2 mm. Two high-purity indium or gold foils of the same diameter and thickness of 0.0025 mm and 0.125 mm, respectively, were attached to the front and back side of the sphere for incident neutron fluence determination. To eliminate the effect of thermal neutrons which unavoidably fill the target room once MeV neutrons strike the walls, floor, and ceiling, the ^{136}Xe cell and the monitor foils were enclosed by a 0.5 mm thick cylindrical cage made out of cadmium, as shown in Fig. 1. The distance between the center of the ^{136}Xe sphere and the end of the neutron production cell was 10 mm. In this figure the experimental setup refers to the measurements done with the deuterium gas cell used for initiating the ^{2}H$(d,n)^{3}$He reaction. The gas cell is 3 cm long and was pressurized to 3 atm of high-purity deuterium gas. A 6.5 mm Havar foil separates the gas from the accelerator vacuum. Typical incident deuteron

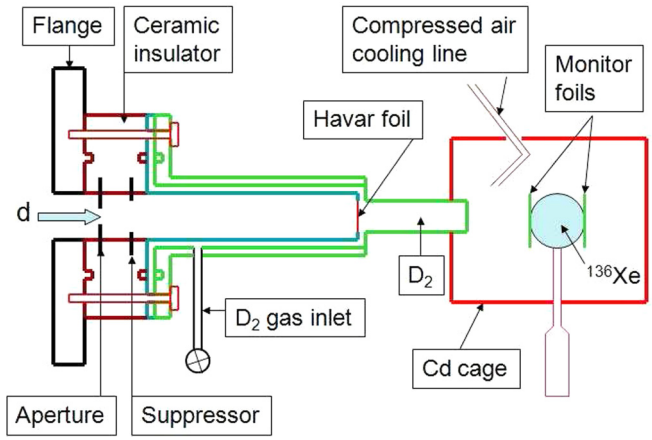

FIG. 1. (Color online) Schematic of experimental arrangement for ^{136}Xe$(n,\gamma)^{137}$Xe cross-section measurements using the ^{2}H$(d,n)^{3}$He reaction.

beam currents were 2 μA. Once the deuteron energy exceeds 2.225 MeV, the deuterons can beak up on the entrance collimator, the Havar foil, or the tantalum beam stop, resulting in lower-energy neutrons (so-called breakup neutrons) than the primary neutrons of interest from the ^{2}H$(d,n)^{3}$He reaction. Therefore, for primary neutrons of energies greater than 5.5 MeV, the incident neutron beam is contaminated by lower-energy neutrons, which also can capture on ^{136}Xe and the monitor foils. In these cases, auxiliary measurements were performed with the deuterium gas pumped out. The incident deuteron beam charge deposited on the deuterium gas cell was used for normalization purposes for these two types of experiments. No attempts were made to produce neutrons of energy greater than 7.8 MeV with the ^{2}H$(d,n)^{3}$He reaction. In this case the incident deuteron energy exceeds 4.45 MeV, and the deuteron breakup can occur in the deuterium gas as well, making it very difficult to account properly for the effect of the associated lower-energy neutrons. Unfortunately, other suitable neutron production reactions in the energy range between 8 and 14 MeV are not available or cannot be initiated with the facilities available at TUNL.

The tritiated titanium target used in connection with the ^{3}H$(p,n)^{3}$He reaction is similar to the one described in Ref. [4] for the ^{3}H$(d,n)^{4}$He reaction. It consists of 2.1 Ci of ^{3}H loaded into a 2.2-mg/cm^{2}-thick layer of titanium of 16 mm diameter, which in turn is evaporated on a 0.4-mm-thick copper backing. Once the incident proton energy exceeds about 2.8 MeV, which corresponds to a primary neutron energy of greater than 2 MeV, the primary neutrons from the ^{3}H$(p,n)^{3}$He reaction are accompanied by low-energy neutrons originating from (p,n) reactions on the titanium and copper backing. Therefore, in the case of $E_n = 2.74$ and 3.34 MeV, auxiliary measurements were performed with an untritiated but otherwise identical target. The two individual measurements were normalized to the accumulated proton charge. Typical proton beam currents were 3.5 μA.

The tritiated target described above was also used for the ^{3}H$(d,n)^{4}$He reaction to produce 14.79 MeV neutrons. In order to take advantage of the narrow 106 keV resonance, the TUNL tandem accelerator was operated at its lowest usable potential of 1 MV and the resulting deuteron beam was energy degraded in the Havar foil to exploit the ^{3}H$(d,n)^{4}$He resonance with its 0° cross section of 415 mb. Breakup neutrons are not produced due to the low incident-deuteron energy. The deuteron current was limited to 3.0 μA to avoid overheating of the Havar foil.

A liquid-scintillator-based neutron detector, positioned at 0° relative to the incident proton or deuteron beam direction at a distance of about 3 m from the neutron production target, was used to monitor the neutron flux. This neutron monitor was also essential in determining the mean neutron energy. For this purpose the incident charged-particle beam was pulsed at a repetition rate of 2.5 MHz with overall time resolution of 2.5 ns. From the measured neutron time of flight, the neutron energy was deferred.

As has been stated above, the ^{136}Xe cell was surrounded by a cage made out of cadmium. The isotope ^{113}Cd has a large neutron absorption edge located at 30 meV that effectively absorbs thermal neutrons. In addition, by using a ^{235}U fission chamber in connection with a pulsed neutron beam, it was shown [11] that the effect of room return neutrons of higher energy than thermal is negligible at the location of ^{136}Xe sphere. Auxiliary neutron-capture experiments were done on natural indium in the 0.5 to 5 MeV energy range, and excellent agreement was found between the cross-section values obtained and the literature value of ^{115}In, supporting the conclusion that room-return neutrons are not an issue in the large neutron time-of-flight (NTOF) target room of TUNL.

The half-life of ^{137}Xe is 3.82 minutes [12]. Therefore, the neutron irradiation time was limited to 15 minutes. The neutron flux was maintained constant throughout irradiation. Depending on energy, the neutron flux at the location of the ^{136}Xe sphere varied between 1×10^{7} and 9×10^{7} n cm^{-2} s^{-1}. Following irradiation, the activity induced in the ^{136}Xe sphere and the monitor foils was measured with well-shielded

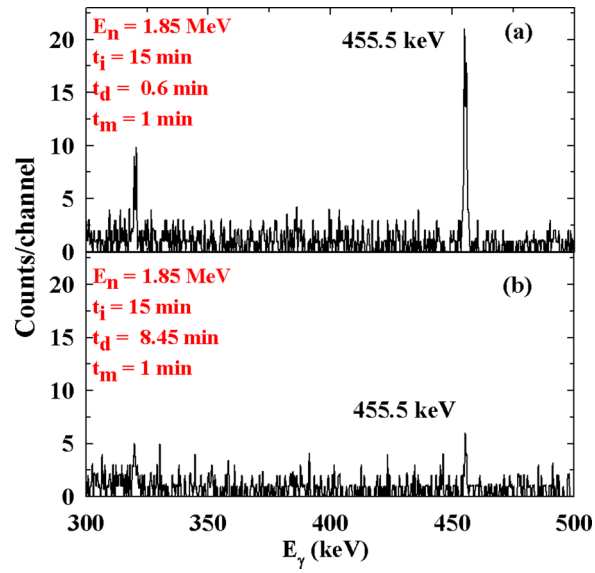

FIG. 2. (Color online) Portion of γ-ray spectra collected for the ^{136}Xe target after activation with 1.85 MeV neutrons.The γ-ray line at 455.49 keV associated with the decay of ^{137}Xe is indicated.

TABLE I. Relevant data for the ^{136}Xe$(n,\gamma)^{137}$Xe reaction along with those of the reference reactions.

Nuclear reaction	Isotopic abundance %	Q value (MeV)	Half-life	γ-ray energy (keV)	γ-ray intensity (%)
^{136}Xe$(n,\gamma)^{137}$Xe	99.9	4.025	3.818 (13) min	455.490 (3)	31
^{115}In$(n,n')^{115m}$In	95.71	−0.34	4.486 (4) h	336.241 (25)	45.8 (22)
^{197}Au$(n,\gamma)^{198}$Au	100	6.512	2.6947 (3) d	411.80205 (17)	95.62
^{197}Au$(n,2n)^{196}$Au	100	−8.072	6.1699 (6) d	355.73 (5)	87

high-purity germanium (HPGe) detectors of 60% relative efficiency. To reduce the transfer time from the irradiation site to the counting site to typically 30 s, the ^{136}Xe HPGe station was mounted just outside of the NTOF target room, while the monitor foils were counted in TUNL's low-background counting facility. The data-acquisition hardware consisted of Canberra 2216 main amplifiers, the Multiport II system, and the associated GENIE 2K software, all provided by Canberra [13]. The energy calibration and the determination of the photopeak detection efficiency of the HPGe detectors were performed with ^{56}Co, ^{60}Co, ^{133}Ba, ^{137}Cs, and ^{152}Eu sources of known activity placed at the same distance as the ^{136}Xe sphere and monitor foils. The energy resolution of the detectors was about 1.8 keV at the 1332 keV γ-ray line of ^{60}Co.

The characteristic γ-ray radiation of 455.49 keV from the deexcitation of ^{137}Xe was used for determining the cross section of the ^{136}Xe$(n,\gamma)^{137}$Xe reaction. The intensity of this γ-ray line was measured in about two minute intervals over a time period of more than three half- lives. Figure 2 shows a typical γ-ray spectrum of the activated ^{136}Xe sphere acquired just after irradiation [Fig. 2(a)] and after 8.5 minutes [Fig. Fig. 2(b)], each for a measuring time of 1 minute. In order to check whether any γ-ray lines from the activation of the structural material (mainly titanium) of the ^{136}Xe sphere are in the region of interest, auxiliary neutron activation measurements were done with an identical, but empty titanium sphere. No γ-ray lines were found that interfere with the 455.49 keV line of ^{137}Xe.

Table I summarizes the reactions studied in the present work along with the relevant quantities needed to obtain the cross section of interest. The half-life times of the reaction products were also derived from the present measurements and were found to be in good agreement with the literature values [12]. Figure 3 gives an example for ^{137}Xe irradiated with 3.34 MeV neutrons. The peak areas of the γ-ray lines of interest were obtained by using the peak fitting software TV [14].

The capture cross section σ was then calculated from the activation formula [15]

$$A = N\sigma\phi\epsilon I_\gamma(1 - e^{-\lambda t_i})e^{-\lambda t_d}(1 - e^{-\lambda t_m}), \qquad (1)$$

where the induced activity A is the total yield in the photopeak, N is the number of target nuclei, ϕ is the neutron flux per square centimeter and second obtained from the monitor reaction, λ is the decay constant of the residual nucleus, ϵ is the photopeak efficiency for the γ-ray energy of interest, I_γ is its branching ratio, t_i is the irradiation time, t_d is the decay time between the end of irradiation and the beginning of offline counting, and t_m is the measuring time. The correction factor for variation in the neutron flux [16] was found to be negligible because the beam intensity was constant throughout the irradiations.

The absolute neutron fluence at the position of the ^{136}Xe sphere was determined from the induced activity in the indium and gold monitor foils. The ^{115}In$(n,n')^{115m}$In reaction was used for incident neutron energies between 0.85 and 7.31 MeV. Cross-section values were obtained from Ref. [17]. The ^{197}Au$(n,\gamma)^{198}$Au reaction was used at 0.37 MeV with the cross section taken from Ref. [18]. Finally, the reaction ^{197}Au$(n,2n)^{196}$Au was employed at 14.79 MeV. In this case the cross section of Ref. [19] was used. The second column of Table II provides the cross-section values for the monitor reactions used in the present work.

Because of the tight geometry of the experimental setup shown schematically in Fig. 1, the fluence at the position of the ^{136}Xe sphere is not simply the average of the fluences obtained from the two monitor foils. In addition, the average neutron energy is not the nominal neutron energy calculated at 0° from the charged-particle energies provided by the accelerator, the energy losses in the target, and the Q values involved, or obtained from the 1.5-inch-diameter and 1.5-inch-long neutron monitor referred to above. Monte Carlo calculations were performed to calculate the neutron fluences at the location of the monitor foils. After normalizing to the experimental values, the Monte Carlo calculations gave the average neutron fluence within the ^{136}Xe sphere and the average neutron energy of the neutron flux striking the sphere. For simulating the experimental setup, information about the angular distribution of the three neutron production reactions used in the present work was obtained from Refs. [20,21]. The attenuation of the

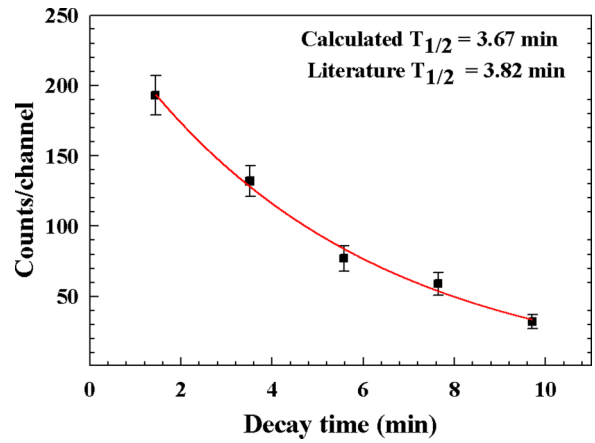

FIG. 3. (Color online) Decay curve for the 455.49 keV γ-ray line of ^{137}Xe measured at $E_n = 3.34$ MeV.

TABLE II. Neutron energy and energy spread, monitor reaction cross-section values used, and ^{136}Xe$(n,\gamma)^{137}$Xe cross-section results obtained in the present work.

Neutron energy $E_n \pm \triangle E_n$ (MeV)	Monitor reactions σ (mb)	^{136}Xe$(n,\gamma)^{137}$Xe σ (mb)
0.37 ± 0.11	170 ± 5.1	0.61 ± 0.08
0.85 ± 0.11	38.93 ± 1.60	0.74 ± 0.08
1.30 ± 0.12	130.23 ± 3.13	1.00 ± 0.12
1.85 ± 0.12	238.71 ± 5.73	0.70 ± 0.07
2.74 ± 0.15	344.40 ± 8.09	0.59 ± 0.08
3.34 ± 0.15	336.66 ± 7.91	0.96 ± 0.22
4.10 ± 0.62	318.20 ± 7.48	1.09 ± 0.11
5.66 ± 0.39	341.90 ± 8.89	0.89 ± 0.09
6.24 ± 0.36	347.62 ± 11.47	0.62 ± 0.09
7.31 ± 0.30	345.04 ± 11.39	0.57 ± 0.16
14.79 ± 0.08	2166.16 ± 23.40	0.73 ± 0.07

neutron flux in the upstream monitor foil, the walls of the titanium sphere, and in the ^{136}Xe gas was taken into account in the Monte Carlo simulations when calculating the neutron flux within the sphere, at the downstream monitor foil, and at the location of the neutron monitor. The average neutron energies and associated energy spread obtained from the Monte Carlo calculations for the geometry used in the present work are given in the first column of Table II. For the data obtained with the ^{3}H$(p,n)^{3}$He reaction, the total neutron energy spread is governed by the reaction kinematics due to the relatively large solid angle subtended by the xenon sphere. In the case of the ^{2}H$(d,n)^{3}$He reaction, the energy loss of the deuteron beam within the deuterium gas cell is responsible for the large majority of the total neutron energy spread. Finally, for the ^{3}H$(d,n)^{4}$He reaction, the width of the 106 keV resonance determines the total neutron energy spread.

Monte Carlo simulations were also performed to correct for the geometry difference between the γ-ray calibration sources used for determining the efficiency of the HPGe detectors and the ^{136}Xe sphere and the associated monitor foils. The attenuation of the 455.49 keV γ rays through the 0.2 mm wall thickness was taken into account as well.

As has been mentioned already, lower-energy neutrons are produced when the ^{3}H$(p,n)^{3}$He reaction is used for producing primary neutrons of energies greater than 2.0 MeV, and when the ^{2}H$(d,n)^{3}$He reaction is used for generating neutrons exceeding 5.5 MeV of energy. The auxiliary measurements performed gave correction factors for the yield of the ^{115}In$(n,n')^{115m}$In reaction at neutron energies of 2.74 and 3.34 MeV of 0.98 and 0.90, respectively. For the ^{136}Xe$(n,\gamma)^{137}$Xe reaction, the correction factor at 2.74 MeV was 1.00, while at 3.34 MeV the correction factor was 0.81. Using the ^{2}H$(d,n)^{3}$He reaction at 6.24 and 7.31 MeV, the measured yield correction factors for the ^{115}In$(n,n')^{115m}$In reaction were 1.00 and 0.97, respectively, while for the ^{136}Xe$(n,\gamma)^{137}$Xe reaction the correction factors were 1.00 and 0.89, respectively. In assigning uncertainties to these correction factors, the yield obtained from the auxiliary measurements was given an estimated 10% uncertainty on top of its statistical uncertainty.

TABLE III. Uncertainty budget for ^{136}Xe$(n,\gamma)^{137}$Xe and monitor reaction cross-section values.

Uncertainty	Xe (%)	Monitors (%)
Counting statistics	5–24	0.6–11
Reference cross sections		1–4.1
Detector efficiency	3–5	1.5–4.5
Source geometry and self-absorption of γ ray	8	0.3–4
Half-life	<1	<0.1
γ-ray intensity		<5
Neutron flux fluctuation	<1	<1
Lower-energy neutrons	<10	<10

The cross-section results obtained for the ^{136}Xe$(n,\gamma)^{137}$Xe reaction in the energy range between 0.4 and 14.8 MeV are given in the third column of Table II. The uncertainty budget of the present data is summarized in Table III. As can be seen, the uncertainty is dominated by statistics. The next largest uncertainty is associated with the subtraction of the lower-energy neutron contribution at $E_n = 2.74$, 3.34, and 7.31 MeV. Figure 4 shows our data (triangles) and the previously existing datum (circle) at $E_n = 1$ MeV from Ref. [10].

In the energy range between 0.4 and 14.8 MeV the cross section is of the order of 1 mb or somewhat lower. The comparison of our data to the Evaluated Nuclear Data Libraries ENDF/B-VII.1 [22] and TENDL-2012 [23] shows that TENDL consistently predicts a larger cross section than obtained in the present work. ENDF/B-VII.1 is in excellent agreement with our data below 2 MeV and in good agreement at 14.79 MeV but predicts considerably lower cross-section values between 3 and 7.5 MeV.

The present work provides, for the first time, experimental cross-section results for the ^{136}Xe$(n,\gamma)^{137}$Xe reaction in the neutron energy range between 1 and 14.8 MeV. The data are important to test theoretical models and to

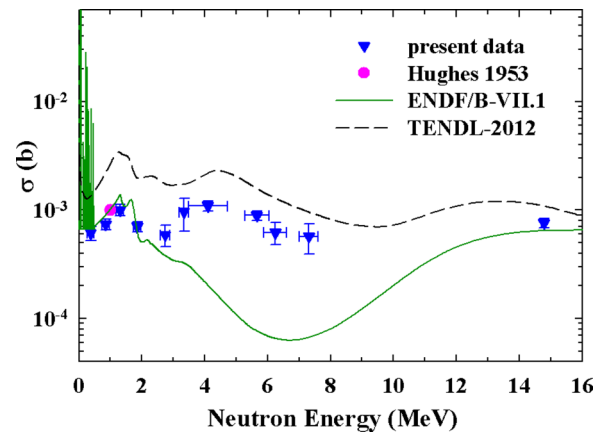

FIG. 4. (Color online) Excitation function of the ^{136}Xe$(n,\gamma)^{137}$Xe capture cross section. The horizontal bars indicate the neutron energy spread. The shaded area below 0.5 MeV is part of the ENDF/B-VII.1 evaluation.

improve evaluations needed to obtain reliable estimates for neutron-induced backgrounds in currently running and future larger-scale experiments aimed at searching for $0\nu\beta\beta$ of ^{136}Xe.

We thank Christopher Romig, Technical University Darmstadt, Germany for providing the ^{136}Xe filled and empty titanium sphere and Anton P. Tonchev for help with the efficiency determination of the HPGe detectors used in the present work. We also acknowledge the contribution of S. W. Finch and M. E. Gooden. This work was supported partially by the US Department of Energy, Office of Nuclear Physics, under Grant No. DE-FG02-97ER41033, and by the National Nuclear Security Administration under the Stewardship Science Academic Alliance Program through the US Department of Energy Grant No. DE-NA0001839.

[1] M. Auger *et al.*, Phys. Rev. Lett. **109**, 032505 (2012).
[2] A. Gando *et al.*, Phys. Rev. Lett. **110**, 062502 (2013).
[3] J. Barea, J. Kotila, and F. Iachello, Phys. Rev. C **87**, 014315 (2013); and references therein.
[4] C. Bhatia, S. W. Finch, M. E. Gooden, and W. Tornow, Phys. Rev. C **87**, 011601(R) (2013).
[5] E. Kondaiah, N. Ranakumar, and R. W. Fink, Nucl. Phys. A **120**, 329 (1968).
[6] M. Bresesti, F. Cappellani, A. M. Del Turco, H. Neumann, and E. Orvini, J. Inorg. Nucl. Chem. **27**, 1175 (1965).
[7] http://www.nndc.bnl.gov/exfor, accession no. 11849014.
[8] J. Macnamara and H. G. Thode, Phy. Rev. **80**, 296 (1950).
[9] H. Beer *et al.*, Astrophys. J. **375**, 823 (1991).
[10] D. J. Hughes, R. C. Garth, and J. S. Levin, Phy. Rev. **91**, 1423 (1953).
[11] C. Bhatia *et al.*, Nucl. Instrum. Methods A (to be published).
[12] NUDAt2, The NUDAT program for Nuclear data on the web, National Nuclear Centre, Brookhaven National Laboratory, version 2.6, available on the internet at http://www.nndc.bnl.gov/nudat2/
[13] http://www.canberra.com.
[14] J. Theuerkauf, S. Esser, S. Krink, M. Luig, N. Nicolay, O. Stauch, and H. Wolters, Program TV, Institute for Nuclear Physics, University of Cologne (1993) (unpublished).
[15] M. Bhike, A. Saxena, B. J. Roy, R. K. Choudhury, S. Kailas, and S. Ganesan, Nucl. Sci. Eng. **163**, 175 (2009).
[16] P. Reimer, Ph.D. thesis, University of Cologne, 2002 (unpublished).
[17] A. B. Smith, S. Chiba, D. L. Smith, J. W. Meadows, P. T. Guenther, R. D. Lawson, and R. J. Howerton, ANL/NDM-115 (1990).
[18] A. N. Davletshin, E. V. Teplov, A. O. Tipunkov, S. V. Tikhonov, and V. A. Tolstikov, Vop. At. Nauki i Tekhn., Ser. Yadernye Konstanty **1**, 13 (1993).
[19] K. I. Zolotarev *et al.*, INDC(NDS)-526 (2008).
[20] H. Liskien and A. Paulsen, At. Data Nucl. Data Tables **11**, 569 (1973).
[21] M. Drosg, DROSG-2000, PC database for 56 neutron source reactions, documented in the IAEA report IAEA-NDS-87 Rev. 5 (2000).
[22] M. B. Chadwick *et al.*, Nucl. Data Sheets **112**, 2887 (2011).
[23] A. J. Koning, S. Hilaire, and M. C. Duijvestijin, in *Proceedings of the International Conference on Nuclear Data for Science and Technology*, Santa Fe, USA, AIP Conf. Proc. No. 769, edited by R. C. Haight, M. B. Chadwick, T. Kawano, and P. Talou (AIP, New York, 2005), p. 1154.